N95-10677

303645

EFFECTIVE UV RADIATION FROM MODEL CALCULATIONS AND MEASUREMENTS

Uwe Feister and Rolf Grewe

Deutscher Wetterdienst
Meteorologisches Observatorium Potsdam
Telegrafenberg, O-1561 Potsdam, Germany

ABSTRACT

Model calculations have been made to simulate the effect of atmospheric ozone and geographical as well as meteorological parameters on solar UV radiation reaching the ground. Total ozone values as measured by Dobson spectrophotometer and Brewer spectrometer as well as turbidity were used as input to the model calculation. The performance of the model was tested by spectroradiometric measurements of solar global UV radiation at Potsdam. There are small differences that can be explained by the uncertainty of the measurements, by the uncertainty of input data to the model and by the uncertainty of the radiative transfer algorithms of the model itself. Some effects of solar radiation to the biosphere and to air chemistry are discussed. Model calculations and spectroradiometric measurements can be used to study variations of the *effective* radiation in space and time. The comparability of action spectra and their uncertainties are also addressed.

1. INTRODUCTION

Solar UV radiation affects the biosphere, some types of materials and the chemistry of atmospheric trace gases (UNEP 1989, 1991). Due to its dependence on atmospheric ozone, cloudiness and turbidity natural and anthropogenic variations of those parameters can alter the diversity of living species, the air quality in the planetary boundary layer and the climate of the earth. For effects with known action spectra the *effective* radiation can be determined from model calculations and/or measurements of the spectral distribution of solar radiation.

2. MODEL CALCULATION OF THE EFFECTIVE SOLAR UV RADIATIATION

A modified version of the radiation model by Green et al. (1974 a, b, 1980) and Schippnick and Green (1982) has been applied to simulate solar UV radiation falling on a horizontal or spherical plane in the UV region using a stepwidth of $\Delta\lambda = 1$ nm. Depending on location and time of the year, solar zenith angles and distances between the earth and the sun were determined from the algorithms given by Sonntag (1989). The extraterrestrial radiation was taken from CIMO (1981), corresponding to a solar constant of
1367 W m^{-2}, and the ozone absorption coefficients from Bass and Paur (1985). Values of the effective radiation E_x (Θ, z, A) for an effect X were determined by

$$E_x(\Theta, z, A, \tau) = \int_0^{\infty} \varepsilon(\lambda)\, E(\lambda, \Theta, z, A, \tau)\; d\lambda$$

(λ: wavelength, Θ: solar zenith angle, z: height, A: surface albedo, τ: optical depth of aerosol and gaseous absorbers). ε (λ) is the normalized action spectrum of a biological effect X, and E (λ, Θ, z, A) is the spectral radiation falling on a horizontal plane. It should be noted that there are doubts that action spectra can really describe biological effects. On the other hand, action spectra are an excellent tool to simulate the radiation environment and its changes at least to a first approximation. Equation (1) can also be used to determine the photolysis rate in [s^{-1}] of a photodissociation process. In that case we have

$$\varepsilon(\lambda) = \varphi(\lambda) \cdot \sigma(\lambda)$$

with the absorption cross section σ (λ) of the gas and the quantum yield φ (λ) of the photodissociation process. In that case, E (λ, Θ, z, A) is the radiation falling on a sphere.

Fig. 1 shows the *radiation amplification factors* RAF determined from model calculations for UVB radiation and for some effects of UV radiation. The RAF is defined here as the percentage change of effective UV radiation for a 1 % ozone reduction. It can be seen that the RAF depends on the ozone concentration in a non-linear manner, and it also depends on the solar zenith angle (not shown). Therefore, the latitudinal and seasonal effects of ozone changes on daily totals of the effective solar UV radiation reaching the surface should be estimated by model calculations carried out for typical average conditions and assumed changes of atmospheric parameters. Effects with a longer tail of the action spectrum at wavelengths in the UVA, such as erythemal and photocarcinogenetic radiation, show a "saturation effect", i.e. a slight decrease of the RAF values with higher total ozone values.

With σ (λ) in eq. (2) as the absorption cross section of ozone (Bass and Paur 1985) and φ (λ) the quantum yield (Aleksandrov et al. (1982), equation (1) was applied to determine the photolysis rate of ozone dissociation

$$O_3 + h\nu \dashrightarrow O(^1D) + O_2(^1\Delta_g) \qquad \lambda < 320\ nm,$$

which is important for the production of the hydroxyl radical from water vapour in the lower troposphere

$$O\,(^1D) + H_2O \dashrightarrow 2\ OH.$$

Fig. 2 shows the modelled dependence of the O_3 photolysis rate on total ozone and on height above the surface. Due to aerosol absorption, which is strongest in the lower troposphere, the strong increase in upward scattering of the radiation from air molecules and aerosols with height, and due to the decreasing attenuation of solar radiation with increasing height, the photolysis rate increases by two orders of magnitude, with the strongest increase occurring in the lowest 1000 m above the surface. For a decrease of total ozone from 400 D to 200 D the O_3 photolysis rate increases by a factor of 3 to 4.

3. MEASUREMENTS OF SOLAR RADIATION

A spectrometer OL 752/10 (Optronic Laboratories) was used for measurements of solar radiation at Potsdam. The instrument is a double monochromator with dual holographic gratings that allow a spectral resolution of 1.5 nm to 10 nm halfwidth. The spectrometer was calibrated by a 200 W tungsten filament lamp, which is abolutely calibrated against an Eppley Standard Cell at the National Institute of Standards and Technology (NIST). The spectroradiometric accuracy of the calibration relative to NIST is given as ± (2...4)%. Due to a straylight problem below 295 nm radiance values with λ < 295 nm had to be extrapolated from radiances measured at higher wavelengths. The spectrometer was placed on the tower roof platform of the Observatory at a height of 18 m above the ground. A spectral resolution of 1.5 nm was selected with a stepwidth of 2 nm. Fig. 3 shows a spectrum measured on October 11, 1991. The time of measurements corresponds to a solar zenith angle of around 60°. Also shown in Fig. 3 is the result of the model calculation for the respective zenith angle. Atmospheric total ozone, which is needed as input to the model, was taken from measurements with a Dobson spectrophotometer (ADDS) and a Brewer spectrometer (DS) at Potsdam. The measured ozone value was decreased by 2.7 % to account for the inadequate ozone absorption coefficients that were in use before January 1, 1992 (Hudson et al. 1991). The model calculation is thus in two ways based on the Bass and Paur (1985) ozone absorption coefficients. It can be seen from Fig. 3 that the correspondence between model calculation and measurement is quite good.

Erythemal radiation $[W\ m^{-2}]_{BBV}$	Rel. to BGBl. (1987)	Reference of action spectrum
0.0194	0.69	Coblentz and Stair (1934)
0.0171	0.60	Berger et al. (1968)
0.0257	0.91	Cripps and Ramsay (1970)
0.0159	0.56	Komhyr & Machta (1973)
0.0188	0.66	DIN (1979)
0.0283	1.00	BGBl (1987)
0.0266	0.94	Photocarcinogenesis (CIE 1986)

Table 1 Erythemal radiation determined for a spectrum of measured solar global radiation, Θ = 59.63°, O_3 = 271 D

However, the uncertainties in the *effective* radiation depend both on the uncertainties in the measured and modelled solar radiation, and on the uncertainties of the action spectrum. As an example, Table 1 shows the erythemal radiation determined from one spectrum of solar global radiation (cf. Fig. 3), but using erythemal action spectra from different sources. For comparison, the last row in Table 1 shows the result for the photocarcinogenesis. It can be seen that the radiation producing photocarcinogenesis is closest to the latest erythemal action spectrum used (BGBl 1987). The different shapes of the action spectra of the erythemal effect do not only provide different absolute values of the erythemal radiation, but do also produce different dependencies of the effective radiation on atmospheric ozone. If model calculations and measurements are to be compared, there must be a consensus on the action spectra applied.The model has been used to simulate variations of the effective radiation in space and time. As an example, Table 2 shows the percentage ratios of daily totals of UV radiation on June 21, September 23, and December 21, referred to March 21, at the station Arkona. Seasonal averages of total ozone (March: 400 D, June: 360 D, September: 310 D, December: 320 D) and typical surface albedo values of 5 %, 5 %, 5 % (grassland) and 60 % (snow) were used as representative input values. While UV and UVA radiation, which are nearly independent on atmospheric ozone, show a seasonal variation from 20 % to 200 % of the spring time value, the seasonal variations of those effects that are strongly ozone dependent are much higher. They extend from 6 % (winter) to 402 % (summer) for the UVB radiation up to the range 2 % to 950 % of the spring time value for photoconjunctivitis. This phenomenon is similarly reflected in the spatial changes of the radiation effects that can be expected as a result of changes in the total ozone concentration. Fig. 4 shows the modelled percentage increase in zonal averages of UVB radiation and in photoconjunctivitic radiation for a global uniform reduction of total ozone by 10 %. In the first model run (no change), the average latitudinal ozone distribution from London et al. (1976) was used. The vertical distribution of ozone is not changed in the calculation, because such a change could produce different results (Brühl and Crutzen 1989). While the latitudinal gradient for UVB is between 10 % in the tropics to around 30 % at high latitudes in winter, for the photoconjunctivitis, which is highly ozone dependent, the range of changes is between 32 % in the tropics to 60 % at high latitudes. It must be noted here that the *absolute* increase in the effective radiation attains its maximum value in the tropics, where the normal radiation levels are highest. On the other hand, the extent to living matter depends on how much additional effective radiation can be tolerated by the individual species and how they are capable of adapting to it.

	June 21	Sept. 23	Dec. 21
UV (λ < 400 nm)	219	101	18
UVA (315<λ<400)	217	100	19
UVB (λ<315 nm)	402	140	6
Erythema (DIN 1979)	488	154	6
Photocarcinogenesis (CIE 1986)	499	156	6
Bactericide (DIN 1979)	716	192	3
Pigmentation (DIN 1979)	221	101	18
Plant response (Caldwell 1971)	606	178	3
Conjunctivitis (DIN 1979)	950	229	2
Photokeratitis (DIN 1979)	385	136	7
Yellowing of PVC (Andrady and Searle 1989, Andrady et al. 1989)	244	105	15

Table 2 Percentage ratios of daily totals of solar global radiation for different effects at the station Arkona (54° 41' N, 13° 26' E) on June 21, September 23, and December 21, referred to March 21

4. CONCLUSION

Effects of solar radiation to the biosphere can be studied both by model calculations and measurements. The uncertainties in both approaches do not only arise from inaccurate algorithms, uncertainties of the input parameters to the radiation model and measurement errors, but also from the uncertainties of the action spectra, which describe an "average" or typical behaviour of an individuum or a group of species under definite conditions. The different types of erythemal action spectra, which produce different values of erythemal radiation, are an example of the increasing

knowledge about radiation effects to human skin.
Despite the deficiencies of the approach to use model calculations and spectroradiometric measurements for estimating the effective radiation, they provide an opportunity to study the effects of solar radiation and its changes to different kinds of living species as well as on air chemistry.

References

Aleksandrov, E. L., I. L. Karol', L. R. Rakipova, J. S. Sedunov, A. Ch. Chrgian (1982), Atmosfernyj ozon i izmenenija global'nogo klimata. Gidrometeoizdat

Andrady, A. L., N. D. Searle (1989), J. Appl. Polymer Sci. 37, 2789 - 2802

Andrady, A. L., A. Torikai, K. Fueki (1989), J. Appl. Polymer Sci. 37, 935 - 946

Bass, A. M., R. J. Paur (1985), In: Atmospheric Ozone. D. Reidel Publishing Company, 606 - 616

Berger, D., F. Urbach, R. E. Davies (1968), Proc. 13. Congressus Internationalis Dermatologicae, Munich 1967

BGBl (1987), Bundesgesundheitsblatt 30 (Nr. 1), 19 - 31

Brühl, C., P. J. Crutzen (1989), Geophys. Res. Lett. 16, 7, 703 - 706

CIE (1986), Division 6, Meeting in Budapest 1986

CIMO (1981), Abriged Final Report of the Eights Session. Mexico City. WMO-No 590

Coblentz, W. W., R. Stair (1934), Bureau of Standards Journal of Research 12, 13 - 14

Cripps, D. J, C. A. Ramsay (1970), Br. J. Derm. 82, 584 - 592

DIN (1979), DIN 5031, Teil 10, November 1979, 1 - 8

Green, A. E. S., K. R. Cross, L. A. Smith (1980), Photochemistry and Photobiology 31, 59 - 65

Green, A. E. S., T. Mo, J. H. Miller (1974a), Photochemistry and Photobiology 20, 473 - 482

Green, A. E. S., E. P. Shettle (1974b), Photochemistry and Photobiology 19, 251 - 259

Hudson, R. D., W. K. Komhyr, C. L. Mateer, R. D. Bojkov (1991), Guidance for use of new absorption coefficients in processing Dobson and Brewer spectrophotometer total ozone data beginning 1 January 1992. Letter to operators at ozone stations. December 1991

Komhyr, W. D., L. Machta (1973), In: The perturbed troposphere of 1990 and 2020. CIAP. Dep. Transportation, Washington, D. C.

London, J., R. D. Bojkov, S. Oltmans, J. I. Kelley (1976), Atlas of the global distribution of total ozone. July 1957 to June 1967, NCAR/TN 113 + STR

Schippnick, P. F., A. E. S. Green (1982), Photochemistry and Photobiology 35, 89 - 101

Sonntag, D. (1989), Abhandlungen des MD der DDR, Nr. 143

UNEP (1989), Environmental Effects Panel Report, November 1989

UNEP (1991), Environmental effects of ozone depletion: 1991 update, November 1991

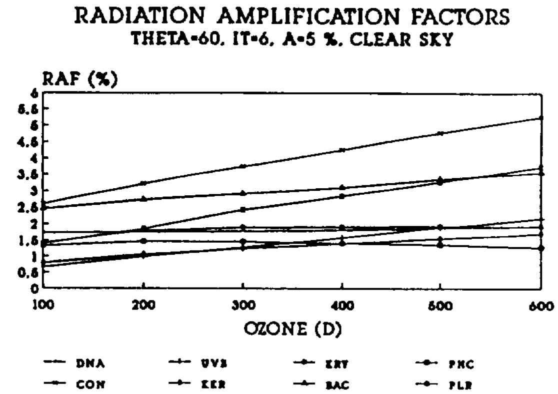

Fig. 1 Radiation amplification factors for biologically effective radiation at the earth's surface in dependence on the total ozone value (DNA: DNA absorption, Sutherland and Griffin 1981; UVB: λ < 315 nm; ERY: erythemal radiation, PHC: photocarcinogenesis; CON: photoconjunctivitis; KER: photokeratitis; BAC: bactericide effect; PLR: plant response). Solar zenith angle: 60°, surface albedo: 5 %, clear sky.

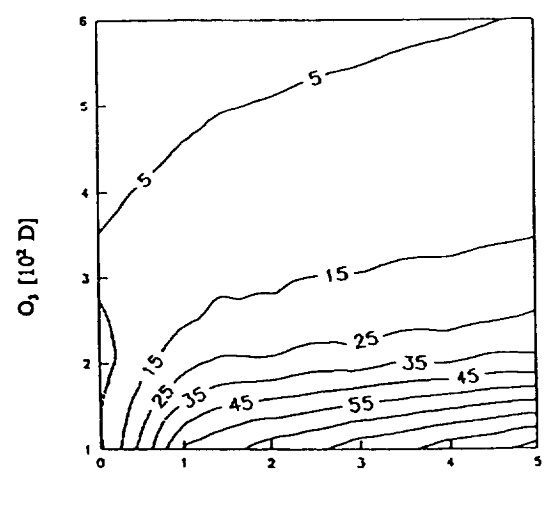

Fig. 2 Photolysis rate of ozone [10^{-6} s^{-1}] in dependence on total ozone for a solar zenith angle of Θ = 60°, surface albedo of 10 %, cloudless conditions and low turbidity

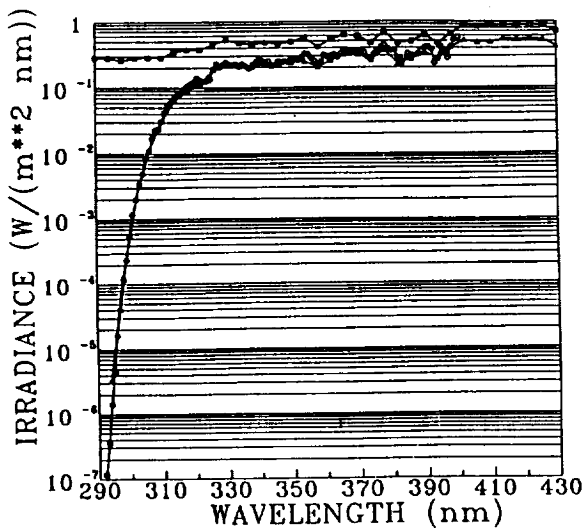

Fig. 3 Solar global radiation at Potsdam (52° 22' N, 13° 5' E) on October 11, 1991, 11.24 CET, Θ = 59.631°
□—□ extraterrestrial radiation from CIMO (1981) corrected for solar zenith angle and distance sun-earth
▲—▲ measurements of global solar radiation taken with the spectrometer OL 752/10 at Potsdam 18 m above the ground, clear sky
○—○ model calculation of global radiation (direct + diffuse) with O_3 = 271 D and an aerosol optical thickness of $\tau = 0.4$ with λ = 350 nm

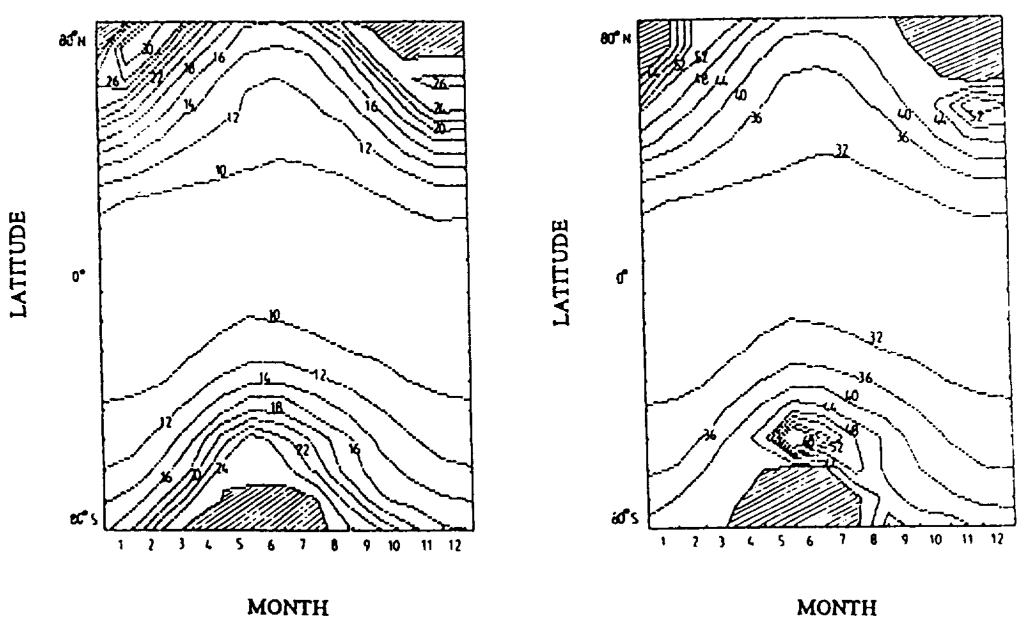

Fig. 4 Latitudinal and seasonal percentage change of UVB (λ < 315 nm) (a) and photoconjunctivitic (b) radiation modelled for a uniform reduction of total ozone by 10 %